THERMAL CONSTRICTION RESISTANCE OF A DISK WITH ARBITRARY HEAT FLUX

A. B. Strong,* G. E. Schneider,† and M. M. Yovanovich‡

University of Waterloo, Waterloo, Ontario

Abstract

Conduction shape factors for a disk on an insulated half-space with arbitrary surface heat flux prescribed have been calculated. The solution of the differential equation was obtained by formulating the problem numerically in the oblate spheroidal coordinate system. The uniform heat flux case and that corresponding to a uniform disk temperature were solved to test the stability and convergence of the numerical solution scheme. Dimensionless resistances were found to be 0.2716 and 0.2507, respectively, which agree to within 1/2% of the analytically known values. In both cases a 40 x 20 grid was chosen, and solutions converged uniformly to the stated accuracy in less than 50 sec IBM 360/75 computing time. Five additional cases were run, and dimensionless resistance values were obtained which lie above and below the bounds formed by the two classical solutions cited previously.

Presented as Paper 74-690 at the AIAA/ASME Thermophysics and Heat Transfer Conference, Boston, Mass., July 15-17, 1974. Financial support of the National Research Council of Canada and the Communications Research Centre, DOC, are gratefully acknowledged.

*Associate Professor, Department of Mechanical Engineering.

†Research Assistant, Department of Mechanical Engineering.

‡Professor, Department of Mechanical Engineering.

Nomenclature

a = disk radius
$A(\lambda a)$ = function, defined by Eq. (3)
C = integration constants or finite-difference coefficients, defined in text
D = constant representing source term in finite-difference equation
i,j = nodal point subscripts in η and θ directions, respectively
I,J = number of spatial divisions in η and θ directions, respectively
J_ν = Bessel function of the first kind of order ν
k = thermal conductivity
P = heat generation/volume/time
P_n = Legendre polynomial of the first kind of order n
q = heat flux
Q = total heat flow rate
Q_n = Legendre polynomial of the second kind of order n
r = radial coordinate
R = overall thermal resistance
R^* = dimensionless overall thermal resistance
T = temperature
v = argument of Q_n, $v \equiv i \sinh\eta$ $(i = \sqrt{-1})$
V = volume
z = axial coordinate

Greek Symbols

η = oblate spheroidal coordinate
θ = oblate spheroidal coordinate
λ = separation constant
μ = argument of P_n, $\mu \equiv \cos\theta$

Introduction

Thermal engineers who need to predict thermal resistance to heat transfer across joints which are lightly loaded and placed in a vacuum environment have been concerned with the problem of accounting for the effect of the microcontact areas. It is commonly assumed that these microcontact areas are circular, have identical diameters, and are uniformly distributed over the apparent contact area. It has been shown by several investigators[1-5] that the dimensionless resistance $R^* \equiv Rka$ is equal to a constant which depends upon the heat flux distribution over the contact area. To date only two cases have been solved: 1) uniform temperature and 2) uniform flux. For

these two cases the dimensionless resistance is equal to 0.2500 and 0.2702, respectively. Further, it often has been assumed by investigators that the uniform temperature and uniform flux boundary conditions yield the minimum and maximum constriction resistances and that all other boundary conditions would result in dimensionless resistances bounded by these values. It is the purpose of this paper to examine heat transfer from circular contact areas having several different heat flux boundary conditions and to resolve the question of whether it is possible to obtain dimensionless constriction resistances outside of the previously noted upper and lower bounds. The resistances will be obtained by means of a finite-difference solution of Laplace's equation expressed in oblate spheroidal coordinates.

Problem Solution

Problem Statement

Consider the resistance to heat conduction from a circular contact area placed on the surface of a half-space. The surface of the half-space outside the contact area ($r > a$) is taken to be perfectly insulated, while over the contact area ($r \leq a$) we will prescribe various heat flux distributions. The temperature within the half-space will tend towards a uniform value at distances large compared with the contact radius. For convenience, it will be assumed that this temperature is zero.

When the temperature field has been determined everywhere in the half-space ($z > 0$) subject to the boundary conditions over the contact area, then the average temperature of the contact area, as well as the total heat flow rate through the contact area, can be calculated, and hence the thermal constriction resistance can be determined.

Analytical Solutions

If circular cylinder coordinates are chosen, then Laplace's equation, assuming axisymmetric heat flux distributions, must be written as

$$(\partial^2 T/\partial r^2) + (\partial T/\partial r)/r + (\partial^2 T/\partial z^2) = 0 \qquad (1)$$

subject to the following boundary conditions:

1) $z = 0$, $0 \leq r \leq a$, one of

   a) temperature is uniform, $T = T_o$
   b) flux is uniform, $q = q_o$

or c) flux is a function of r, $q = q(r)$

2) $z = 0$, $r > a$, surface is insulated, $\partial T/\partial z = 0$

3) $r = 0$, $z > 0$, temperature is finite

4) $\sqrt{r^2 + z^2} \to \infty$, temperature goes to zero (2)

The solution of Eq. (1) requires use of the infinite integral[2]

$$T(r,z) = C\int_0^\infty A(\lambda a)\, e^{-\lambda z}\, J_o(\lambda r)\, \frac{d\lambda}{\lambda} \tag{3}$$

where the constant C and the function $A(\lambda a)$ are to be determined from the boundary conditions along $z = 0$.

The boundary conditions specified over $r \leq a$ and $r \geq a$ result in dual infinite integrals which must be solved simultaneously for C and $A(\lambda a)$. Solutions are available only for the uniform temperature and uniform flux cases.[2,§] For case 1, $C = 2T_o/\pi$ and $A(\lambda a) = \sin(\lambda a)$, whereas, for case 2, $C = aq_o/k$ and $A(\lambda a) = J_1(\lambda a)$. The dimensionless constriction resistances have been determined for these two cases to be 1/4 and $8/3\pi^2$, respectively. The theory of dual infinite integrals has not yet been developed to the point where solutions for other boundary conditions can be determined readily.

A great simplification in the analysis of the case of uniform temperature can be obtained by use of oblate spheroidal coordinates (η,θ). By means of the following transformations[6]

$$r = a\,\cosh\eta\,\sin\theta,\quad z = a\,\sinh\eta\,\cos\theta \tag{4}$$

Eq. (1) becomes

$$(\partial^2 T/\partial\eta^2) + \tanh\eta\,(\partial T/\partial\eta) + (\partial^2 T/\partial\theta^2) + \cot\theta\,(\partial T/\partial\theta) = 0 \tag{5}$$

which is valid for axisymmetric temperature distributions. The parameter η ranges from $\eta = 0$ on the disk to $\eta = \infty$ corresponding to distances large compared with the disk radius. The other parameter, θ, ranges from $\theta = 0$, corresponding to the 0z axis, to $\theta = \pi/2$, corresponding to $z = 0$, $r > a$.

---

§ Because of recent developments at the University of Waterloo, two additional analytic solutions have been found for a cosine and cosine-squared flux distribution. These latest results are incorporated in Table 1 of this work but are not reported in detail here.

For the isothermal boundary condition, Eq. (5) reduces to

$$(\partial^2 T/\partial \eta^2) + \tanh\eta\ (\partial T/\partial \eta) = 0 \tag{6}$$

whose solution can be shown to be

$$T = C_1 + C_2 \cot^{-1}(\sinh\eta) \tag{7}$$

Equation (7) with $C_1 = 0$ and $C_2 = 2T_o/\pi$ satisfies the mixed boundary conditions along $z = 0$. The heat flux distribution over the disk can be calculated and is

$$q = 2\ k\ T_o/\pi\ a\ \cos\theta = 2\ k\ T_o/(\pi\sqrt{a^2 - r^2}) \tag{8}$$

By means of Eq. (8), the total heat flow rate can be shown to be

$$Q = 4ka\ T_o \tag{9}$$

According to the definition of thermal constriction resistance and Eq. (9), the dimensionless resistance is 1/4. It is evident that, for this case, using a more natural set of coordinates has resulted in a great simplification of the thermal problem.

The constant flux boundary condition, as well as the variable flux boundary conditions, will result in a two-dimensional temperature field, at least near the contact area. For these cases we must write $T = T(\eta,\theta)$ and use Eq. (5) to describe thermal equilibrium within $z > 0$. The solution of Eq. (5) obtained by the method of separation of variables can be expressed in the following form [6]:

$$T(\eta,\theta) = \sum_{n=0}^{\infty} C_n\ Q_n(v)\ P_n(\mu) \tag{10}$$

where Q_n is the Legendre polynomial of the second kind whose argument is $v = i\sinh\eta$, and P_n is the Legendre polynomial of the first kind of argument $\mu = \cos\theta$. Solutions based upon Eq. (10) are not available at present.

Finite-Difference Formulation

As a result of the problems associated with obtaining an analytic solution for other than the most simple of disk boundary conditions, a numerical solution was sought. In this analysis the method of finite differences was used. If the finite-difference spatial discretization of the governing differential equation is performed in either the circular cylinder or Cartesian coordinate system, the discontinuity of the surface flux distribution occurring at the disk outer edge gives rise to considerable numerical difficulty, since the second-order truncation error inherent in the expansion of the

conduction equation cannot adequately approximate the large adjustment of the thermal flow field required in the vicinity of this discontinuity.

The finite-difference equation to be used in the approximation of Eq. (5) can be derived by two independent methods. The first involves performing a Taylor series expansion to second order on the differential Eq. (5). The second method, the one used for this analysis, is to perform an energy balance on a control volume of finite dimensions. With this control volume centered about a point in space characterized by the notation (i,j), i and j shall be used to indicate the finite discretization of space in the η and θ directions, respectively. For uniform spacing in each direction independently, successive nodes are incremented in the η and θ directions by amounts $\Delta\eta$ and $\Delta\theta$, respectively. Note that these increments do not represent the physical distances separating adjacent nodes but merely the change in the respective coordinate value between these nodes.

The energy balance for the steady-state problem must then provide a zero net energy addition to the control volume. This is accomplished by a balance of the heat flow rates entering or leaving this control volume through the control volume surfaces. For the axisymmetric thermal loading conditions considered here, there will be four such heat flow rates. $Q_{i-\frac{1}{2},j}$, for example, represents the heat flow rate in the positive i or η direction across the control surface located along the η coordinate corresponding to a discretized location $i-\frac{1}{2}$. The energy balance is then, for steady-state operation with a total source strength $P\Delta V$, given simply by

$$Q_{i-\frac{1}{2},j} - Q_{i+\frac{1}{2},j} + Q_{i,j-\frac{1}{2}} - Q_{i,j+\frac{1}{2}} + P\Delta V = 0 \qquad (11)$$

By using first central difference quotients between nodes to approximate first derivatives, a linkage is set up whereby the central nodal temperature becomes related to the temperature at its four (six for complete asymmetry) nearest neighbors (Fig. 1). By collection of common terms, the finite-difference form of the energy balance can be written as

$$C_s T_{i,j} = C_1 T_{i-1,j} + C_2 T_{i+1,j} + C_3 T_{i,j-1} + C_4 T_{i,j+1} + D \qquad (12)$$

where, after some manipulation and division by common factors, the coefficients can be determined to be

$$C_1 = \frac{1}{(\Delta\eta)^2} - \frac{\tanh[(i-\frac{1}{2})\Delta\eta]}{2\Delta\eta} \quad (13a)$$

$$C_2 = \frac{1}{(\Delta\eta)^2} + \frac{\tanh[(i-\frac{1}{2})\Delta\eta]}{2\Delta\eta} \quad (13b)$$

$$C_3 = \frac{1}{(\Delta\theta)^2} - \frac{\cot[(j-\frac{1}{2})\Delta\theta]}{2\Delta\theta} \quad (13c)$$

$$C_4 = \frac{1}{(\Delta\theta)^2} + \frac{\cot[(j-\frac{1}{2})\Delta\theta]}{2\Delta\theta} \quad (13d)$$

$$C_s = \sum_{n=1}^{4} C_n \quad (13e)$$

$$D = \frac{P\Delta V}{2\pi ka \cosh\eta \sin\theta \, \Delta\eta \, \Delta\theta} \text{ or equivalent source term} \quad (13f)$$

where the η-coordinate at node (i,j) is given by $[(i-\frac{1}{2})\Delta\eta]$ and the θ-coordinate by $[(j-\frac{1}{2})\Delta\theta]$.

Boundary Conditions

Having determined the nodal coefficients for the generalized internal node, we now turn our attention to those nodes for which the surrounding control volume has one or more surfaces contacting physical boundaries of the total thermal system. The boundary control volumes (C.V.) of concern in this analysis and their associated thermal boundary conditions are illustrated in Figs. 2a-2d. Internodal links which do

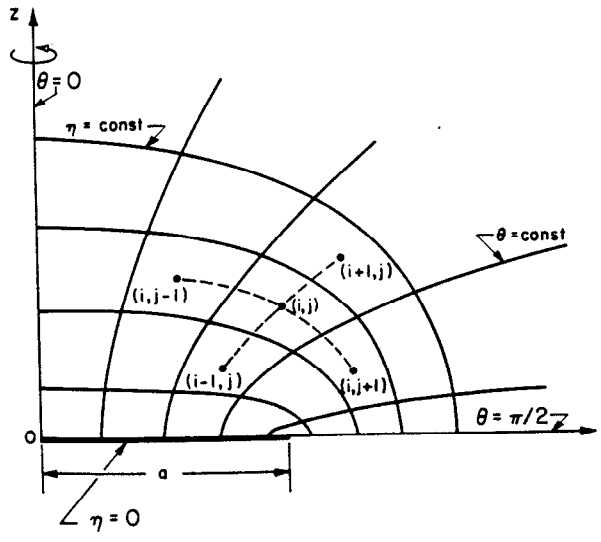

Fig. 1 The coordinate system and numerical molecule definition.

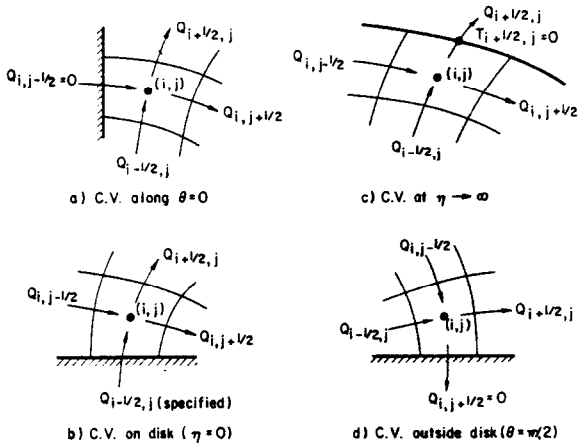

Fig. 2 Boundary control volumes (C.V.) used in boundary condition specification.

not cross a boundary will have their associated coefficients unchanged and will not be considered here. The four boundary conditions of direct interest in this problem will now be discussed.

a) $\theta = 0$. Because of the problem symmetry about the vertical axis, the line defined by the equation $\theta = 0$ will represent a zero flux boundary. Since the control volume has been selected such that the surfaces located at $j-\frac{1}{2}$ for $j = 1$ are coincident with this boundary of symmetry (Fig. 2a), this condition is reflected by the equation

$$Q_{i,j-\frac{1}{2}}\Big|_{j=1} = 0 \tag{14}$$

The effect of this condition on the coefficients of Eq. (13) is that we must set

$$C_3 = 0 \tag{15}$$

For the case of no internal heat generation, D will also be zero.

b) $\theta = \pi/2$. This boundary is by the problem description itself another zero flux boundary. Again, because of the coincidence of the control volume surface $j+\frac{1}{2}$ for $j = J$ with the physical boundary, this condition can be expressed, from Fig. 2d, by

$$Q_{i,j+\frac{1}{2}}\Big|_{j=J} = 0 \tag{16}$$

By reasoning similar to that used for the condition at $\theta = 0$, it follows that, to satisfy Eq. (16), we must set

$$C_4 = 0 \tag{17}$$

Again D will be zero.

c) $\eta \to \infty$ ($\eta \simeq 8$). For this boundary, illustrated in Fig. 2c, we are concerned with a prescribed temperature at $\eta = \infty$. It was found numerically and can be illustrated analytically that it is sufficient, for the accuracy of the present solution, to take $\eta = 8$ as the numerical equivalent of $\eta \to \infty$. For convenience, the value $\eta = 8.5$ was used in this analysis. This particular boundary then requires no special treatment other than to insure that the temperature for all nodes $(I + 1, j)$ is assigned and maintained at the appropriate specified value. This has been taken as zero for this analysis but can be arbitrarily selected to be any other value. Again D must be set to zero since there is no internal heat generation.

d) $\eta = 0$. The final condition to be considered is the specified flux condition at $\eta = 0$. These control volumes are typified by that shown in Fig. 2b. Now, since the solution to any problem will be directly dependent on the boundary conditions, it is desirable that boundary conditions be specified as accurately as possible. For this particular problem, since we know the surface flux and by integration the heat flow rate crossing the control surface on the disk, it is better to use the known heat flow rate directly rather than to introduce the error incurred in specifying the surface gradient which can only at best be approximated by difference quotients in the numerical treatment.

The total heat-transfer rate crossing a control surface between $\theta_j - \Delta\theta/2$ and $\theta_j + \Delta\theta/2$ is given by the integral over this control surface,

$$Q_{\frac{1}{2},j} = \pi a^2 \int_{\theta_j - \frac{\Delta\theta}{2}}^{\theta_j + \frac{\Delta\theta}{2}} q(\theta) \sin(2\theta)\, d\theta \tag{18}$$

This heat flow rate represents a rate of heat addition to the control volume, and, since the energy balance, Eq. (11), is a scalar balance, its direction need not be specified. That is, provided heat is added to the control volume in any manner at a rate given by Eq. (18), the energy balance at that node will be satisfied. Perhaps the simplest method of providing this rate of energy addition is to assign to those control volumes a total source strength of equivalent magnitude. This is accomplished by the assignment

$$P\Delta V = \pi a^2 \int_{\theta_j - \frac{\Delta\theta}{2}}^{\theta_j + \frac{\Delta\theta}{2}} q(\theta) \sin 2\theta d\theta \tag{19}$$

from which, for application to Eq. (12), the constant D becomes

$$D = \frac{a}{2k\cosh(\Delta\eta/2)\, \sin\theta_j\, \Delta\theta\Delta\eta} \int_{\theta_j - \frac{\Delta\theta}{2}}^{\theta_j + \frac{\Delta\theta}{2}} q(\theta) \sin(2\theta)\, d\theta \tag{20}$$

Since in this fashion the heat transfer in the positive η direction has been accounted for, it would be redundant to include the nodal temperature linkage of nodes (1,j) and (0,j). Consequently we set

$$C_1 = 0 \tag{21}$$

with

$$C_s = \sum_{n=1}^{4} C_n$$

as before.

Numerical Solutions

So that we might establish confidence in the numerical solution employing oblate spheroidal coordinates, the two boundary conditions for which classical analytical solutions are available were examined: 1) the uniform temperature case, and 2) the uniform flux case. Agreement is excellent in both cases, with approximately 0.5% error when a 40 x 20 grid arrangement was used. To further establish this confidence and to become familiar with the numerical characteristics of this problem, the constant flux case was examined in greater detail. This was done with a 20 x 10 grid for which the resulting solution is within 2% of the true value. All solutions were obtained by successive iteration over the field using an over-relaxation factor of 1.5. Figure 3 depicts the convergence characteristics for the problem. It is seen that the maximum percent change between iterations of the field temperature based on the average temperature over the field monotonically decreases with increasing number of iterations. Convergence was assumed when this maximum percent change, $(\Delta T/\bar{T})_{max} \times 100$, was less than 0.05. It is seen from Fig. 3 that convergence of the resistance value occurs much earlier in the computation. The resulting 2% error is attributed to the truncation error of a 20 x 10 grid. It has been assumed on the basis of these results that, for other flux distributions with identical grid sizing and convergence criteria, a comparable accuracy in our solution is to be expected. For a 40 x 20 grid arrangement, this error is reduced to approximately 0.5%. This truncation error dependence on grid size is illustrated in Fig. 4, where the dimensionless resistance, $R^* \equiv Rka$, has been plotted to display the dependence on $\Delta\eta$. The more minor influences of the grid spacing in the θ direction are shown by the curve parameter $\Delta\theta/\Delta\eta$. The relatively

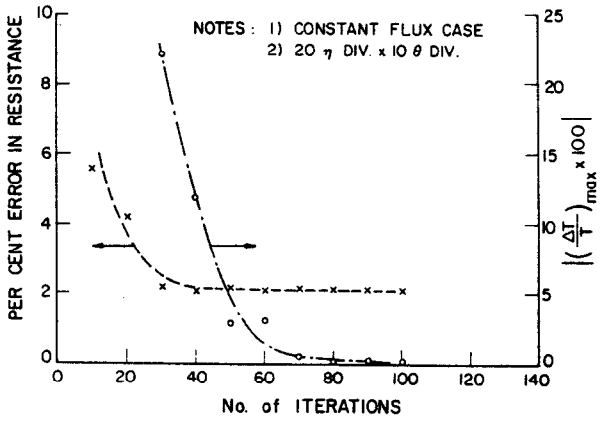

Fig. 3 Effect of number of iterations on resistance error and on the maximum change in temperature between successive iterations.

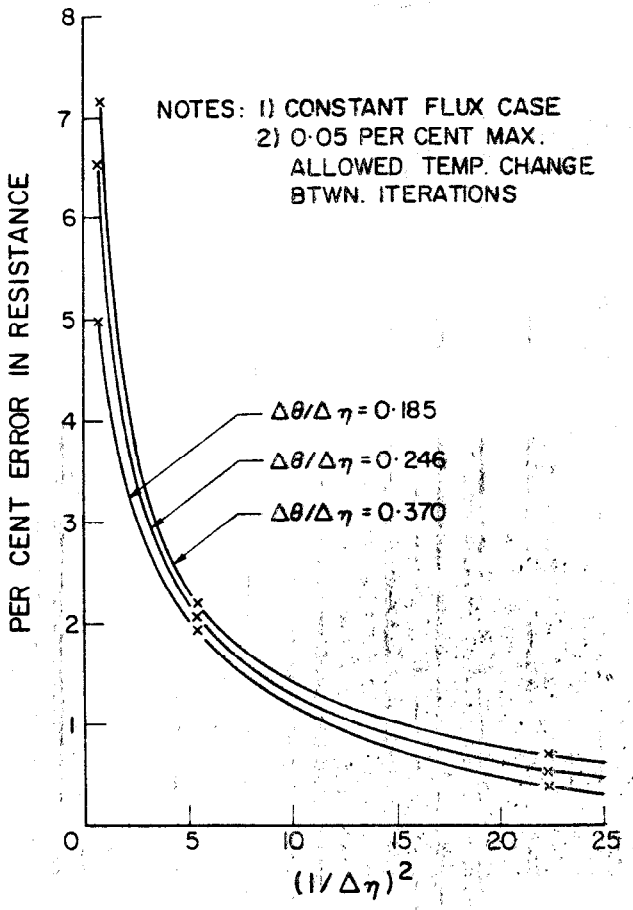

Fig. 4 Effect of grid size on error in resistance.

minor effect of this parameter suggests that in oblate spheroidal coordinates the heat flow behavior is predominantly one-dimensional in η, with small variations occurring in the θ direction. These results then confirm our previous suspicions that advantages similar to those obtained by using oblate spheroidal coordinates in the analytic solution of the isothermal disk case can be realized by using this coordinate system in the numerical formulation of the problem.

Results

After having established a level of confidence in the numerical solution of this problem, we are now prepared to examine arbitrary flux distributions over the disk. Flux distributions were selected on the basis that Eq. (18) be integrable analytically in addition to requiring that a spectrum of possible disk flux distributions be examined. In this fashion, it was possible to examine distributions in which flux concentrations appear at the disk center and outer edge in addition to intermediate locations. Although not required for the analysis, the multiplicative constant was adjusted so that the total thermal loading of the system would be the same for all cases considered, since this permits a direct comparison of field and surface temperatures. The various flux distributions are shown graphically in Fig. 5, where they are plotted as a function of the spheroidal coordinate θ. With these distributions, the integral of Eq. (18) was evaluated and the result used as input to the solution program. The field temperatures were then computed, surface temperatures found, the average surface temperature evaluated, and, based on the total heat flow rate, the dimensionless thermal resistance can be determined. The results obtained for the flux distributions considered are presented in Table 1. Where analytical solutions are known, the computational error is evaluated.

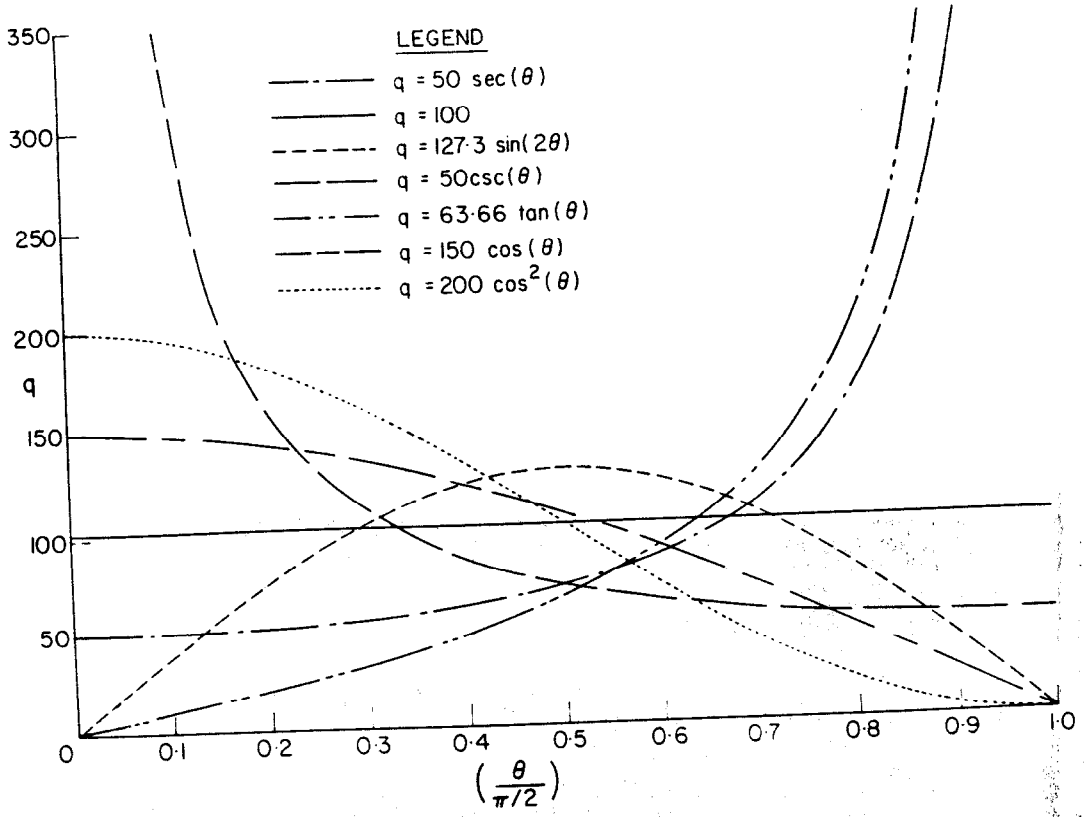

Fig. 5 Disk heat flux distributions.

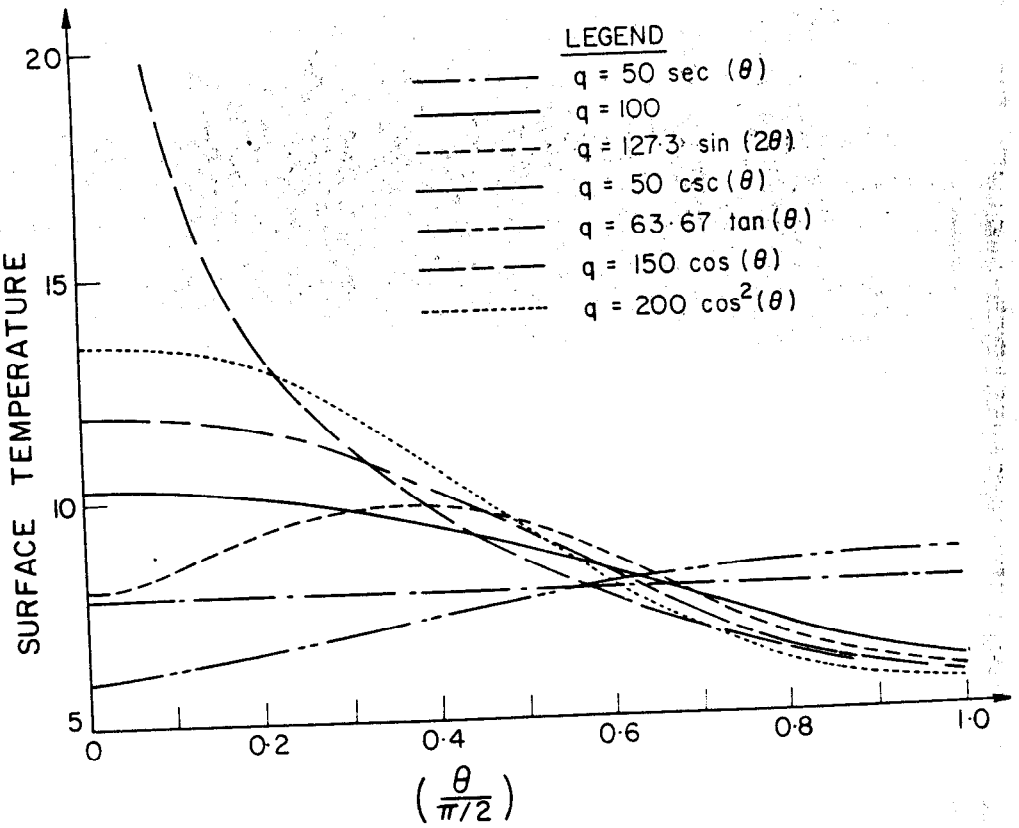

Fig. 6 Variation of disk temperature for the cases considered.

Table 1 Results and comparison of R^*

$q(\theta)$	Exact	Present	Percent error	Grid sizing (η-div.x θ-div.)	Computational time (IBM 360/75), sec
$q = 50 \sec(\theta)$ (isothermal)	0.2500	0.2507	0.3	40x20	48
$q = 100$	0.2702	0.2716	0.5	40x20	47
$q = 50 \csc(\theta)$	...	0.2889	...	40x20	96
$q = 127.3 \sin(2\theta)$	...	0.2773	...	20x10	20
$q = 63.67 \tan(\theta)$	...	0.2422	...	20x10	18
$q = 150 \cos(\theta)$	0.2813	0.2850	1.3	40x20	183
$q = 200 \cos^2(\theta)$	0.2882	0.2922	1.4	40x20	183

The surface temperature distributions resulting from each of the imposed flux distributions are shown graphically in Fig. 6. Area weighted average surface temperatures have been used in the evaluation of R^*.

Conclusions and Discussion

One conclusion which might be drawn from this work, though not the primary objective of the research, is that the appropriate choice of coordinate system for the numerical analysis is instrumental in keeping the computational time for solution to a minimum. The second and most important conclusion to be drawn from this work, and contrary to some hypotheses in common usage, is that the thermal constriction resistance of this system is not bounded by the values for the uniform temperature and uniform flux cases. We have noted several flux distributions which lead to resistances lying outside of this range. If this work were to be continued, certainly many more such cases could be found.

References

[1]Jeans, J. H., The Mathematical Theory of Electricity and Magnetism, Cambridge University Press, Cambridge, England, 1963, pp. 356-357.

[2]Carslaw, H. S. and Jaeger, J. C., Conduction of Heat in Solids, Oxford University Press, London, 1959, pp. 216-217.

[3]Roess, L. C., "Theory of Spreading Conductance," referenced in "Thermal Resistance Measurement of Joints formed between Stationary Metal Surfaces," by Weills, N. D. and Ryder, E. A.,

Transactions of the American Society of Mechanical Engineers, Vol. 71, 1949, pp. 259-267.

[4]Mikic, B. B. and Rohsenow, W. M., "Thermal Contact Resistance," Rept. DSR74542-41, Contract No. NGR-22-009-065, Sept. 1966, M.I.T. Heat Transfer Laboratory.

[5]Cooper, M. G., Mikic, B. B., and Yovanovich, M. M., "Thermal Contact Conductance," International Journal of Heat and Mass Transfer, Vol. 12, 1969, pp. 279-300.

[6]Moon, P. and Spencer, D. E., Field Theory Handbook, Springer Verlag, Berlin, 1961.